Available online at www.sciencedirect.com
ScienceDirect
Journal of Power Sources 163 (2006) 409–414
JOURNAL OF POWER SOURCES
www.elsevier.com/locate/jpowsour

Short communication

Sintering and electrical properties of $Ce_{0.8}Y_{0.2}O_{1.9}$ powders prepared by citric acid-nitrate low-temperature combustion process

Hongmei Xu, Hongge Yan *, Zhenhua Chen

College of Materials Science and Engineering, Hunan University, Changsha, Hunan 410082, China

Received 12 July 2006; received in revised form 11 September 2006; accepted 15 September 2006
Available online 27 October 2006

Abstract

$Ce_{0.8}Y_{0.2}O_{1.9}$ nanopowders were prepared using a citric acid-nitrate low-temperature combustion process. The effect of pH value of the solutions on the ionization of citric acid and the chelating of metal ions was studied. It was found that when the pH value of the solutions was bigger than 6, the citric acid was completely ionized and the stable complexes were formed between rare earth metal ions and the citric acid. Then the stable gels were obtained. The effect of the amount of oxidants (Φ) on the combustion fashions and combustion reaction time of the gels, the properties of the as-synthesized powders, the sintering behavior of the as-synthesized powders and the conductivity of the sintered pellets was also investigated. The results showed that the green density, sintered density and the ionic conductivity of the specimens increased with Φ. When Φ was equal to 1.5, the powders with good dispersion and compressibility were obtained, and the green density of the powders was 52.5%. The relative density of the sintered sample was over 95% at 1350 °C for 4 h and the conductivity of the sintered specimen was 0.034 S cm^{-1} at 700 °C.

Keywords: Yttria-doped ceria; Electrolyte; Low-temperature combustion synthesis; Sintering; Conductivity

1. Introduction

Doped ceria is a promising alternative solid electrolyte to yttria stabilized zirconia (YSZ) in solid oxide fuel cell (SOFC) application [1–3]. Its higher oxygen ion conductivity and lower interfacial losses with cathode and anode will bring down the SOFC operating temperature to 500–800 °C. The lower operating temperature has a lot of benefits, such as cheaper components materials, lower degradation problems, less thermal mismatch and wider choice of sealing materials [4].

The synthesis of nanosized, low-agglomerated doped ceria powders is of immense importance to get dense sintered product at a lower temperature, because it is well known that CeO_2 based materials are difficult density below 1600 °C by the conventional solid-state reaction method [5–7]. The wet-chemical synthesis of high reactive powders has been proved to be one of the most effective routes to decrease the sintering temperature of ceramic materials. A wide variety of methods have been used for the production of nanosized ceramic powders, such as co-precipitation [8], hydrothermal synthesis [9], polymerized complex process [10,11], and sol–gel [2]. Most of these methods involve complicated steps and expensive raw materials to fabricate nanosized ceria-based ceramic powders.

A gel low-temperature combustion synthesis method shows some advantages mainly to due its lower-cost raw materials, fewer steps and better control of stoichiometry while producing powders in the nanometer range. Gel-combustion routes are based on the gelling of the solutions and subsequent combustion of the gels between the salts of the desired metals (usually nitrates) and some organic fuels, such as alanine, citric acid, glycine, etc. [12–14]. Compared with other organic fuels, citric acid is cheaper, the reaction is wilder and can be controlled more easily. The aim of this paper was to synthesize nanoscaled $Ce_{0.8}Y_{0.2}O_{1.9}$ (abbreviated as YDC) powders with good properties by a citric acid-nitrates gel-combustion route and improve the sinter ability of the as-burnt powders and the conductivity of the sintered YDC. The effect of the pH value of the solutions on the ionization of citric acid and the chelating of metal ionic and the effect of the amount of the oxidants on the gel-combustion behavior, particle size distribution and agglomeration of the yttria-doped powders were investigated. Densification of the

* Corresponding author. Tel.: +86 731 8821648; fax: +86 731 8821648.
E-mail address: xyzh7@sina.com (H. Yan).

0378-7753/$ – see front matter © 2006 Elsevier B.V. All rights reserved.
doi:10.1016/j.jpowsour.2006.09.021

green pellets and the conductivity of the sintered ceramics were also discussed.

2. Experimental procedure

2.1. Sample preparation

A gel low-temperature combustion synthesis was used to prepare the powders of YDC ceramics. Analytical-grade $Ce(NO_3)_3{\cdot}6H_2O$ (≥99%), Y_2O_3 (≥99.99%), NH_4NO_3, ammonium hydroxide and citric acid were used as raw materials. $Ce(NO_3)_3{\cdot}6H_2O$ and Y_2O_3 were weighed according to the molar ratio in YDC. Y_2O_3 was first dissolved in warm (approximately 60 °C) diluted nitric acid and then mixed together with $Ce(NO_3)_3{\cdot}6H_2O$ in deionized water. Citric acid was added in a proportion of 1.5 per mol metal ions. The amount of oxidants (Φ) was changed by adding NH_4NO_3, and Φ is equal to n_R/n_I, where n_I is the amount of oxidants which makes the citric acid combust theoretically as follows:

$$0.8Ce(NO_3)_3{\cdot}6H_2O + 0.2Y(NO_3)_3 + 1.5C_6H_8O_7 + 6NH_4NO_3 \rightarrow Ce_{0.8}Y_{0.2}O_{1.9} + 9CO_2 + 7.5N_2 + 22.8H_2O$$

and n_R is the amount of oxidants used in the experiments. In the experiments, NH_4NO_3 was added in n_R/n_I at 0.5, 1 and 1.5. The pH value of the solution was adjusted by adding ammonium hydroxide. The translucent solutions were evaporated at 80 °C to form the viscous gels. Then the viscous gels were ignited at 400 °C in a pre-heated furnace. Depending on the "Φ" value, different fashions of thermal decomposition reactions were started. The system was homogenous during the whole process and no precipitation was observed.

Nanosized powders were uniaxially pressed into the 13-mm-diameter pellets at 200 MPa. The pellets were sintered at the temperature range of 1200–1400 °C for 4 h with a heating rate of 5 °C/min.

2.2. Sample characterization

The ionization of citric acid and the chelating of metal ions were investigated by an Infrared spectroscopy (IR, Nicolet-510, America). Simultaneous TG/DTA (NETZSCH STA449C, Germany) experiments were performed on part of the dried gel precursors in order to study the combustion process. Temperature ranges of analysis were from room temperature to 600 °C with a heating rate of 10 °C/min in a flowing air atmosphere. The as-burnt powders were characterized by X-ray diffraction (XRD) (Cu Kα, Siemens D5000 (Germany)) to identify the existing phases and estimate grain sizes (d_{XRD}). Grain sizes of the as-burnt powders were calculated by the X-ray line broadening technique performed on the (2 2 0) diffraction of CeO_2 lattice from the Scherrer education:

$$d_{XRD} = \frac{K\lambda}{\beta\cos\theta} \quad (1)$$

where θ is the Bragg angle of diffraction lines, K is the a shape factor ($K = 0.9$ in this work), λ is the wavelength of incident X-rays (0.15406 nm), and β is the corrected half-high width given by

$$\beta^2 = \beta_m^2 - \beta_s^2 \quad (2)$$

where β_m is the measured half-high width and β_s is the half-high width of a standard CeO_2 sample with a known crystallite size of larger than 200 nm.

The specific surface area (S_{BET}, $m^2\ g^{-1}$) of the as-synthesized powders was measured by the standard Brunauer-Emmett-Teller (BET) technique with N_2 adsorption using a Monosorb (Quanta Chrome, America). The specific surface area was converted into average particle size (d_{BET}) according to the following equation assuming that the particles are closed spheres with smooth surface and uniform size:

$$d_{BET} = \frac{6 \times 10^3}{d_{th} S_{BET}} \quad (3)$$

where d_{th} is the theorical density of the material (g cm^3). Assuming that the dopants are homogeneously distributed in the CeO_2 structure and occupy the Ce^{4+} sites to form a solid solution, the d_{th} values can be calculated according to:

$$d_{th} = \frac{4[(1-x)M_{Ce} + xM_Y + (2-x/2)M_O]}{a^3 N_A} \quad (4)$$

where a is the lattice constant of the YDC materials at room temperature, N_A is the Avogadro constant, and M refers to the atomic weight.

A transmission electron microscope (TEM, Hitachi-800, Japan) was employed for studies of particle characteristics of the as-burnt powders. Laser particle size analyzer was employed to study the average agglomerate size and particle-size distribution. The agglomeration coefficient (ψ) is:

$$\psi = \frac{d_{med}}{d_{BET}} \quad (5)$$

where d_{med} is median radius of the powders, d_{BET} is the average particle calculated according to S_{BET}.

The width of the size distribution (S) is:

$$S = \frac{d_{90} - d_{10}}{d_{50}} \quad (6)$$

where d_{10}, d_{50} and d_{90} is the particles size when the accumulative distribution is 10%, 50% and 90% respectively.

Green density of the compacts was calculated from the mass and dimension of the samples. The sintered density was determined using Archimedes principle. The microstructure of the sintered pellets was investigated using scanning electron microscope (SEM, JSM6700F, Japan). Average grain size was obtained from SEM micrographs using the linear intercept technique.

Silver paste was painted onto both sides of the sintered pellets and fired at 850 °C for 10 min to prepare the electrodes. Then Pt wires were fixed onto the silver electrodes to transfer current. Ionic conductivity of the samples was measured from 300 ° to 700 °C in air by two-probe impedance spectroscopy in the frequency range of 0.1–100 KHz with an applied ac signal of 50 mV using CHI660C.

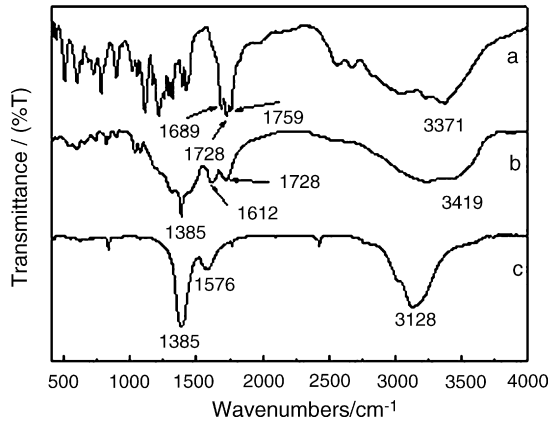

Fig. 1. IR spectra of samples for (a) citric acid; (b) gel under $n_{CA}/n_M{}^{n+} = 1.5$, pH = 2; (c) gel under $n_{CA}/n_M{}^{n+} = 1.5$, pH = 7.

3. Results and discussion

In citric acid-nitrates gel-combustion synthesis, the formation of metal ions-citric acid chelation complexes is the precondition to prevent the separation or precipitation of rare earth metal ions and obtain the homogeneous products. Citric acid (H_3cit) is weak acid, so the pH value of the solutions controls the dissociation of carboxylic acid groups (−COOH) and then affects the formation of metal ions-citric acid complexes. When the pH value is low, citric acid is partially ionized. The metal ions cannot be totally chelated, and there will be free metal ions in the solution. Fig. 1 shows IR spectra of citric acid and the gels with different pH value. In citric acid, the stretching vibration for free carboxyl groups are observed at 1689 cm^{-1}, 1728 cm^{-1} and 1759 cm^{-1} (Fig. 1a). When pH value is equal to 2 (Fig. 1b), except for the band at 1612 cm^{-1}, which represents the stretching vibration for carboxyl ions (COO^-) from metal carboxylates, the band at 1728 cm^{-1}, which represents the stretching vibration for free carboxyl groups (−COOH), still can be observed. This shows citric acid is partially ionized. In the XRD pattern, the diffraction peaks of crystallized phases for metal nitrates can be observed (Fig. 2a) because rare earth metal ions are not totally chelated. The IR peak near 3400 cm^{-1} is due to the O–H stretching associated with the hydroxyl group of remaining water. For pH = 2.5–5, precipitation phases appear, which result from the hydrolysis of the metal ions (Fig. 2b). For pH = 2.5–5, most citric acid is ionized into $(H_2Cit)^-$, and $[RE(H_2Cit)]^{2+}$ was formed between $(H_2Cit)^-$ and rare earth metal ions (RE^{3+}). $[RE(H_2Cit)]^{2+}$ is unstable, and hydrolysis of the metal ions is more stable than $[RE(H_2Cit)]^{2+}$, so the hydrolysis precipitation of the metal ions is formed. When pH > 6, the solution becomes transparent again. Fig. 1c is IR spectrum of the dried gel for pH = 7, and the sorption bands at 1689 cm^{-1}, 1728 cm^{-1} and 1759 cm^{-1} disappear. The sorption band at 1576 cm^{-1} is assigned to the asymmetric stretching of carboxylates ($-COO^-$) from metal carboxylates. In the XRD pattern of the dried gel (Fig. 2c), only the diffraction peaks of NH_4NO_3 are observed, which confirm the total chelating of metal ions [15]. The band at 3128 cm^{-1} in the gel is attributed to the stretching vibrations of the hydrogen-bonded groups. For pH > 6, citric acid is ionized into $(Hcit)^{2-}$, cit^{3-}, and ring complexes $RE(Hcit)^+$, $[RE(Hcit)_2]^-$ and $[RE_2cit_3]^{3-}$ are formed between $(Hcit)^{2-}$, cit^{3-} and RE^{3+}. $RE(Hcit)^+$, $[RE(Hcit)_2]^-$ and $[RE_2cit_3]^{3-}$ are very stable, so the precipitation are revolved and the solutions become transparent again. The pH value of the solutions is 7 in the following experiments.

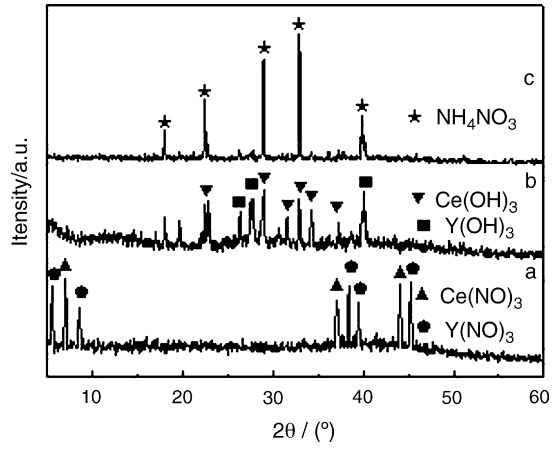

Fig. 2. XRD patters of gels for (a) $n_{CA}/n_M{}^{n+} = 2$, pH = 2; (b) $n_{CA}/n_M{}^{n+} = 1.5$, pH = 4; (c) $n_{CA}/n_M{}^{n+} = 1.5$, pH = 7.

In order to study the effect of the amount of the oxidants on the gel-combustion behavior, the dried gels prepared at different Φ are characterized via TG/DTA at a heating rate of 10 °C/min in static air. The simultaneous TG/DTA curves of the dried gels under $\Phi = 0.5$, 1and 1.5 are shown in Fig. 3. A strong exothermic peak can be clearly seen at about 260 °C, at which the maximum weight loss occurs in all the curves, and the exothermic behavior at about 260 °C corresponds to the auto-ignition step. However, when Φ is equal to 0.5, a multi-step decomposition of precursor is observed and the DTA curve shows two distinct exothermic peaks, related two distinct weight loss steps. The second exothermic step in DTA curve of Fig. 3a is presumably due to the oxidation of some carbonaceous residues. IR spectra are examined to investigate the composition and structure of the as-burnt powders. It is clearly seen that when Φ is equal to 0.5, the absorption bands corresponding to NO_3^-, carboxyl group and O–H group in water molecule still exit. It shows that the reaction between the reductant (citric acid) and the oxidants (nitrates) is not complete when the oxidants are deficient, and the as-burnt powders contain nitrates, carbonaceous residue and water. It is also observed in the experiments that the as-burnt powders are light yellow tinged with dark gray dot when "Φ" value is equal to 0.5, which implies that the reaction is incomplete.

Some characteristics of the powders with different Φ are listed in Table 1. This table clearly shows that the amount of oxidants significantly affects the specific area, grain size, average particle size, width of size distribution as well as agglomeration coefficient. When Φ increases from 0.5 to 1.5, the grain size (d_{XRD}) increases from 5 nm to 15 nm because the quantity of heat in reaction process increases with the amount of oxidants. d_{TEM} is the primary particle size and the primary particles are composed of the grains. The primary particle size shows the same increment tendency as the grain size. d_{SET} is the average particle size calculated from S_{BET}. When hard agglomeration is formed

Table 1
The effect of the amount of oxidants on powder characteristics

Samples (Φ)	Crystalline sizes (nm)			Median radius, d_{med} (μm)	Width of size distribution (ψ)	Agglomeration coefficient (S)	S_{BET} (m^2/g)
	d_{XRD}	d_{TEM}	d_{SET}				
0.5	5	5–25	12.8	1.24	24	96.6	70
1	9	20	35	0.6	16	20	25.4
1.5	15	40	40	0.2	10.4	5	22

between particles, d_{SET} is bigger than d_{TEM}. When Φ is equal to 0.5, the reaction is incomplete and divided into multi-step resulting in a small amount of gas product and long reaction time, so the powders are severe agglomeration and broad distribution in size. Increasing with the oxidant amount, the reaction time becomes shorter and the more gas is produced in the reaction. The gas will prevent the agglomeration of the primary particles. So the powders obtained are narrower size distribution width and less agglomeration coefficient, and d_{SET} is almost the same as d_{TEM}.

For the YDC powders from the different Φ, green density increases with Φ. The green density has great relationship with the powder characteristics under the same consolidation conditions. For the nanopowders, the friction forces between particles are big during compaction due to the large surface areas of the powders, and thus the green density is low. The hard agglomeration of nanocaled powders decreases the density of green bodies pressed from those nanopowders [16], and it needs very big pressure to break the hard agglomeration. The agglomeration coefficient decreases with the increase of the oxidant amount, so the green density of the as-burnt powders increases with the increase of the oxidant amount. The green density of the powders with $\Phi = 0.5$, 1 and 1.5 is 38%, 45% and 52.5%, respectively. The powders with $\Phi = 1.5$ have the highest green density, which is higher 14% related to the density of the bodies made from the powders with $\Phi = 0.5$. Fig. 4 is the effect of Φ on the densification of pellets at different sintering temperature. The sintered density also increases with Φ. The sintered density increases from 80% to 95.1% at 1350 °C for 4 h when Φ increases from 0.5 to 1.5 under the same consolidation conditions. Fig. 5 shows SEM micrographs of the sintered bodies prepared at 1350 °C for 4 h. Fig. 5a is the surface micrograph of the sample prepared from the nanopowders with $\Phi = 0.5$. The average grain size is about 0.4 μm and the specimen exhibits a significant amount of porosity, which results from the existence of large pores in the green body because of agglomerated particles. The pores will

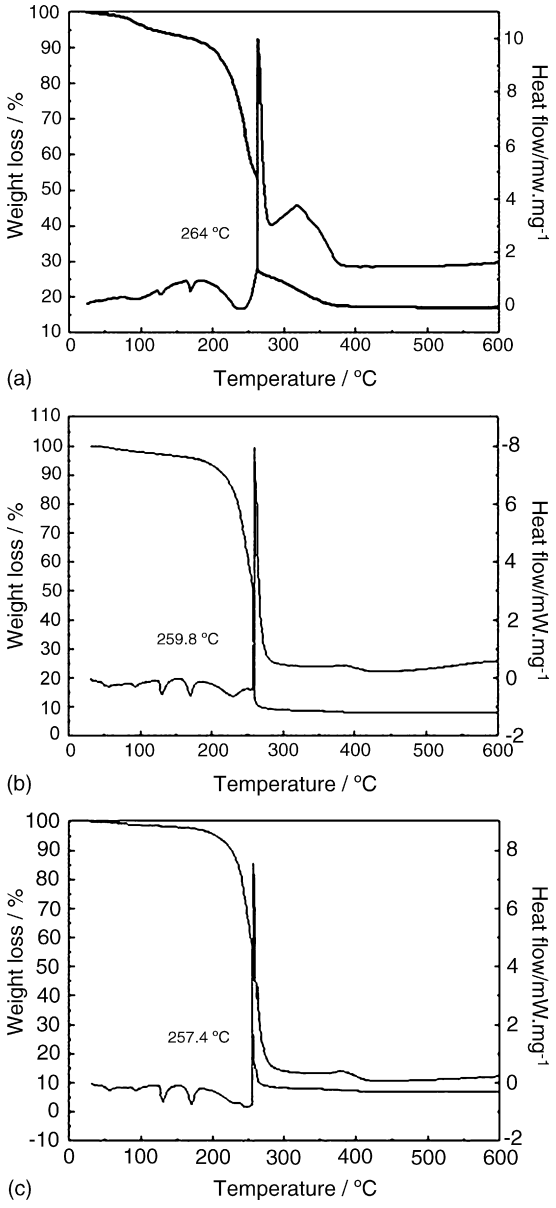

Fig. 3. Simultaneous TG/DTA curves of the dried gel with (a) $\Phi = 0.5$; (b) $\Phi = 1$; (c) $\Phi = 1.5$.

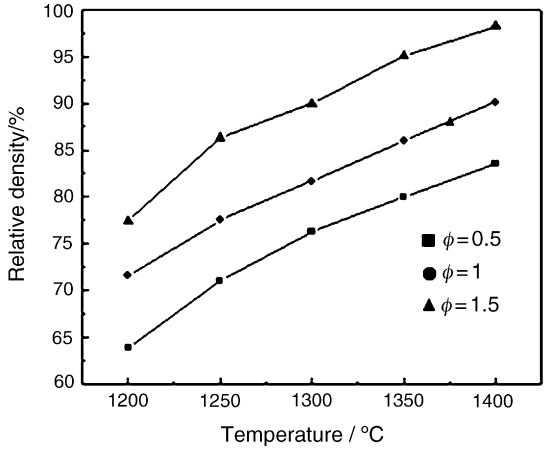

Fig. 4. The effect of "Φ" value on the densification of pellets at different sintering temperature.

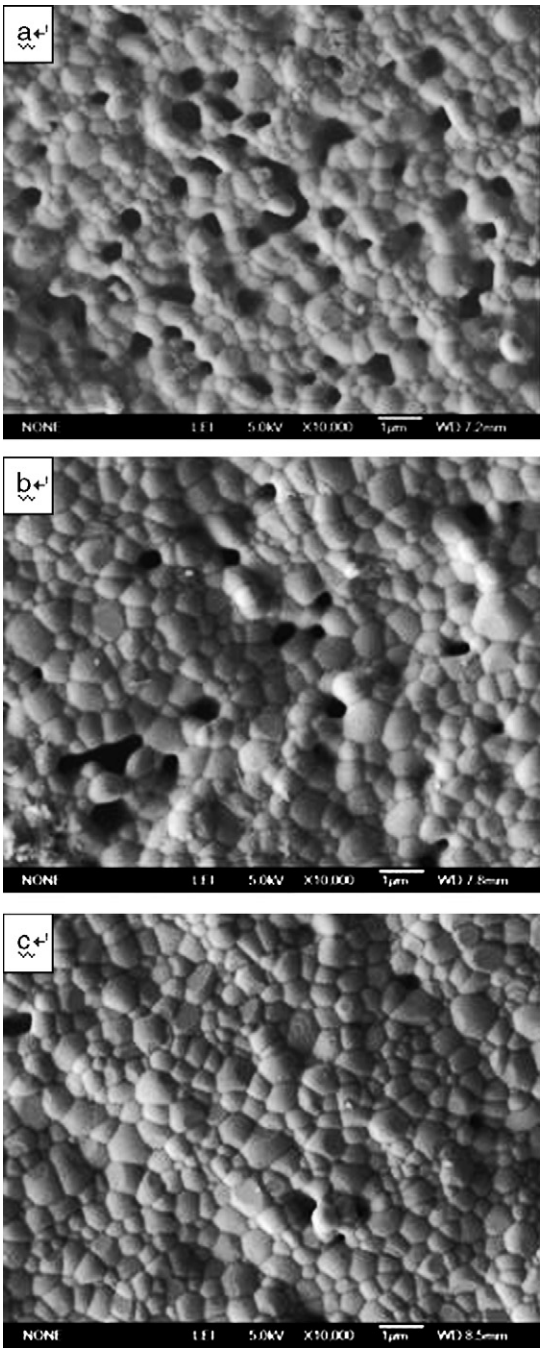

Fig. 5. SEM micrographs of the sintered $Ce_{0.8}Y_{0.2}O_{1.9}$ ceramics at 1350 °C for 4 h (a) $\Phi = 0.5$; (b) $\Phi = 1$; (c) $\Phi = 1.5$.

be difficult to be removed by the sintering process. The residual water in the powders also inhibits the sintering behavior because of the hard agglomeration resulting from the hydrogen-bonded groups among water molecules when the green bodies are heated [17,18] and the gases because of the decomposition of the residual nitrates and carbonaceous also prevent the sintering of the green bodies. The amount of porosity decreases with the increase of "Φ" value. When Φ is equal to 1.5, the sintered body is almost completely dense and the average grain size is only 0.46 μm (Fig. 5c). When Φ is equal to 0.5, the powders obtained are fine and have high sintering activity, but broad

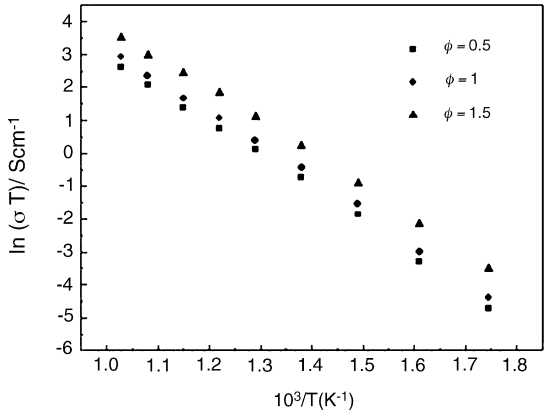

Fig. 6. The Arrhenius plots of specimens for different "Φ" value at 1350 °C for 4 h.

distribution in size, hard agglomeration and low green density result in a comparatively low sintered density after sintering.

The conductivity of sintered specimens is also different with different Φ. Fig. 6 presents the Arrhenius plots for sintered YDC specimens prepared by powders with different Φ at 1350 °C for 4 h. Fig. 6 shows that the conductivity increases with Φ, the conductivity is 0.034 S cm^{-1} at 700 °C when Φ is equal to 1.5 and higher than that in [18]. The increase in conductivity of sintered specimens with Φ may be attributed to the elimination of interconnected porosity, because the porosity in the grain boundary would block the oxygen vacancies mobility [19]. From the Arrhenius plots, the activation energies are 0.89 eV, 0.9 eV, and 0.85 eV, respectively when Φ increases from 0.5 to 1.5. The activation energy of the ceramic with $\Phi = 1.5$ is smaller than that in [20,21].

4. Conclusions

A citric acid-nitrate low-temperature combustion synthesis process was optimized to fabricate well-dispersed yttria-doped ceria nanopowders. The pH value of the solution controls the ionization of carboxylic acid groups of the citric acid. When the pH value of the solution is larger than 6, the citric acid is completely ionized and the stable gel is obtained. The amount of oxidant in the combustion synthesis influences the decomposition of the gels, which in turn affects significantly the particle size, size distribution and agglomeration of yttria-doped ceria powders. Yttria-doped ceria powders produced from $\Phi = 1.5$ are fine (in the nanometer scale), narrow in size distribution and weak agglomeration. When Φ is equal to 0.5 or 1, it results in broad size distribution and hard agglomeration of yttria-doped ceria powders.

Density of the sintered yttria-doped ceria ceramics is mainly influenced by the powders characteristics. When Φ is equal to 0.5 or 1, the hard agglomeration among the yttria-doped ceria powder particles and the residual nitrates, carbonaceous and water in the powders prevent the densification of the yttria-doped ceria green pellets during sintering. When Φ is equal to 1.5, dense yttria-doped ceria ceramics (relative density over 95%) can be produced by sintering at 1350 °C for 4 h.

Because the porosity in the sintered specimens will block the oxygen vacancies mobility, the conductivity of sintered ceramics increases with Φ. The activation energies of 0.89 eV, 0.9 eV, and 0.85 eV respectively are obtained for Φ increasing from 0.5 to 1.5. The conductivity is 0.034 S cm^{-1} at 700 °C when Φ is equal to 1.5.

Acknowledgments

The authors would like to thank the financial support provided by the Natural Science Foundation of China (No. 50304008) and the Doctoral Science Foundation of Ministry of Education (No. 20030532016) and the State Key Laboratory Foundation (No. 2005016).

References

[1] Toshiaki Matsui, Minoru Inaba, Atsushi Mineshige, Zempachi Ogumi, Solid State Ionics 176 (2005) 647–654.
[2] Feng-Yun Wang, Songying Chen, Soofin Cheng, Electrochem. Commun. 6 (2004) 743–746.
[3] J. Ma, T.S. Zhang, L.B. Kong, et al., J. Eur. Ceram. Soc. 24 (2004) 2641–2648.
[4] K. Zheng, B.C.H. Steele, M. Sahibzada, I.S. Metcalfe, Solid State Ionics 86–88 (1996) 1241–1244.
[5] Tian Chunyan, Chan Siuwai, Solid State Ionics 134 (2000) 89–102.
[6] Hiroyuki Yoshida, Kazuhiro Miura, Takehisa Fukui, et al., J. Power Sources 106 (2002) 136–141.
[7] J.F.Q. Rey, E.N.S. Muccillo, J. Eur. Ceram. Soc. 24 (2004) 1287–1290.
[8] S.K. Tadokoro, T.C. Porfirio, R. Muccillo, E.N.S. Muccillo, J. Power Sources 130 (2004) 15–21.
[9] S. Dikmen, P. Shuk, M. Greenblatt, H. Gocemez, Solid State Sci. 4 (2002) 585–590.
[10] M.T. HernaÂ ndez, J.R. Jurado, P. DuraÂ n, J.C.C. Abrantes, F.M.B. Marques, Solid State Ionics 50 (1992) 167–173.
[11] M. Yashima, M. Kakihana, K. Ishii, Y. Ikuma, M. Yoshimura, J. Mater. Res. 11 (1996) 1410–1415.
[12] C. Peng, Y.N. Liu, Y.X. Zheng, Mater. Chem. Phys. 82 (2003) 509–514.
[13] S.V. Chavan, A.K. Tyagi, J. Mater. Res. 19 (2) (2004) 474–480.
[14] D.Y. Chung, E.H. Lee, J. Alloys Comp. 374 (2004) 69–73.
[15] S. Vivekanandhan, M. Venkateswarlu, N. Satyanarayana, Mater. Lett. 58 (7–8) (2004) 1218–1222.
[16] D.G. Lamas, G.E. Lascalea, N.E. WalsoÈ e de Reca, J. Eur. Ceram. Soc. 18 (1998) 1211–1217.
[17] Z.G. Huang, X.D. Sun, Z.M. Xiu, S.W. Chen, C.T. Tsai, Mater. Lett. 58 (2004) 2137–2142.
[18] S.W. Zha, Q.X. Fu, Y. Lang, C.R. Xia, G.Y. Meng, Mater. Lett. 47 (2001) 351–355.
[19] S.K. Tadokoro, T.C. Porfírio, R. Muccillo, E.N.S. MMuccillo, J. Power Sources 130 (2004) 15–21.
[20] T.S. Zhang, J. Ma, H.T. Huang, P. Hing, Z.T. Xia, S.H. Chan, J.A. Kilner, Solid State Ionics 5 (2003) 1505–1511.
[21] C.Y. Tian, S.W. Chan, Solid State Ionics 134 (2000) 89–102.